

## Carbon cycling hysteresis in permeable carbonate sands over a diel cycle: Implications for ocean acidification

Tyler Cyronak,\* Isaac R. Santos, Ashly McMahan, and Bradley D. Eyre

Centre for Coastal Biogeochemistry, School of Environment, Science, and Engineering, Southern Cross University, Lismore, New South Wales, Australia

### *Abstract*

Dissolved inorganic carbon, dissolved oxygen,  $H^+$ , and alkalinity fluxes from permeable carbonate sediments at Heron Island (Great Barrier Reef) were measured over one diel cycle using benthic chambers designed to induce advective pore-water exchange. A complex hysteretic pattern between carbonate precipitation and dissolution in sands and the aragonite saturation state ( $\Omega_{Ar}$ ) of the overlying chamber water was observed throughout the incubations. During the day, precipitation followed a hysteretic pattern based on the incidence of photosynthetically active radiation with lower precipitation rates in the morning than in the afternoon. The observed diel hysteresis seems to reflect a complex interaction between photosynthesis and respiration rather than  $\Omega_{Ar}$  of the overlying water as the main driver of carbonate precipitation and dissolution within these permeable sediments. Changes in flux rates over a diel cycle demonstrate the importance of taking into account the short-term variability of benthic metabolism when calculating net daily flux rates. Based on one diel cycle, the sediments were a net daily source of alkalinity to the water column ( $5.13$  to  $8.84$   $mmol\ m^{-2}\ d^{-1}$ , depending on advection rates), and advection had a net stimulatory effect on carbonate dissolution. The enhanced alkalinity release associated with benthic metabolism and pore-water advection may partially buffer shallow coral reef ecosystems against ocean acidification on a local scale.

Rising atmospheric  $CO_2$  concentrations have the potential to drastically alter biogeochemical cycles occurring in coastal ecosystems. The accumulation of  $CO_2$  in seawater changes the overall composition of dissolved inorganic carbon (DIC) species and lowers the pH (Zeebe and Wolf-Gladrow 2001; Morse and Arvidson 2002). This can have inhibitory effects on numerous biological processes, including marine calcification (Hoegh-Guldberg et al. 2007). Coral reefs are thought to be some of the most susceptible ecosystems to ocean acidification, with future models indicating a complete ecosystem phase shift from corals to algae (De'ath et al. 2009; Veron 2011). In order to understand how ocean acidification will affect coral reef communities it is important to understand how the benthic communities contribute to ecosystem-level biogeochemical cycles.

The precipitation and dissolution of carbonate minerals in marine sediments is thought to be determined by the saturation state ( $\Omega$ ) of the pore water with respect to the metastable mineral (Ku et al. 1999; Yates and Halley 2006). Most studies focusing on the effects of ocean acidification on coral reefs use the aragonite saturation state ( $\Omega_{Ar}$ ) as an indicator of ecosystem health (De'ath et al. 2009; Veron 2011). However, coral reef sediments are made up of a mixture of different carbonate mineral phases, including low magnesium calcites (LMCs), high magnesium calcites (HMCs), and aragonite (Weber and Woodhead 1969). The mineralogy of the carbonate sediments influences solubility such that calcites with higher magnesium content are more soluble than pure calcite and aragonite (Morse and Arvidson 2002; Andersson et al. 2007). As carbonate sediments dissolve they release alkalinity, which can

potentially buffer against decreases in pH due to ocean acidification (Andersson et al. 2005, 2011).

In shallow carbonate sediments, photosynthesis and respiration modify the pH of pore waters (Yates and Halley 2006; Werner et al. 2008), which can potentially influence the precipitation and dissolution of carbonate minerals. Photosynthesis by benthic microalgae takes up  $CO_2$ , which leads to the oversaturation of pore waters and promotes the abiotic precipitation of carbonates as well as calcification by benthic microorganisms (Werner et al. 2008). The production of  $CO_2$  during oxic respiration can drive the dissolution of carbonate sediments and release alkalinity into the pore waters (Ku et al. 1999; Yates and Halley 2006). The advection of seawater through permeable sediments has been shown to have a large effect on the rates of production and respiration in sediments (Janssen et al. 2005; Glud et al. 2008). We suspect that advection also influences the dynamics of carbonate precipitation and dissolution.

Numerous mechanisms act on different temporal and spatial scales to transport seawater through permeable carbonate sediments within coastal ecosystems (Santos et al. 2012). Cycling of water through the sediments can alter the chemistry of the overlying water column, with influx and efflux rates based on residence time, advection rate, sediment chemistry, biological processes, and the initial chemistry of the seawater (Eyre et al. 2008). The advection of overlying waters can replenish oxygen, organic compounds, and dissolved ions within the sediments, causing them to act as biological catalysts, intensifying benthic processes such as respiration (Glud et al. 2008). To date, most studies in carbonate sediments have focused on how advection affects photosynthesis and respiration (Rasheed et al. 2004; Clavier et al. 2008) or nutrient cycling (Eyre et

\* Corresponding author: tcyronak@gmail.com

al. 2008). The dynamics of carbonate precipitation and dissolution in permeable sediments is still poorly understood (Werner et al. 2008; Rao et al. 2012).

Because photosynthesis is affected by multiple physical processes, such as the availability of photosynthetically active radiation (PAR), nutrients, and CO<sub>2</sub>, rates are highly dependent on the time of day and have been shown to undergo hysteresis within corals and algae (Levy et al. 2004). Since benthic photosynthesis and respiration alter the seawater chemistry in permeable carbonate sediments (Glud et al. 2008; Santos et al. 2011), carbonate precipitation and dissolution may undergo hysteresis over a diel cycle. It is expected that precipitation rates would be lower in the morning than in the afternoon as the result of a lowered saturation state caused by nighttime respiration. We hypothesize that carbonate precipitation and dissolution in permeable coral reef sediments will follow a diel hysteresis driven by benthic photosynthesis and respiration. To test this hypothesis we conducted high-resolution time-series observations of advective benthic chambers in permeable carbonate sediments at Heron Island. We also hypothesize that advection will stimulate the dissolution of carbonate sediments and release alkalinity into the water column that may partially buffer against ocean acidification on a local scale.

## Methods

*Study site*—All sampling was performed from 09 through 10 October 2011 along the inner reef flat of Heron Island (23°27'S, 151°55'E) at a similar site to that described in Glud et al. (2008) and Eyre et al. (2008). Heron Island is an offshore coral cay located at the southern end of the Great Barrier Reef, 72 km off of the Australian mainland. The reef flat covers an area of 26.4 km<sup>2</sup>, and roughly 85% is covered by carbonate sands (Glud et al. 2008), with an average depth of 1.7 m (Wild et al. 2004a). Our study site was a sand patch roughly 100 m offshore and east of the marine research station. Sediment grain size was mostly medium to very coarse sand (Wentworth scale), with grain sizes as follows: 12.1% > 2 mm, 30.5% between 1 and 2 mm, 27.3% between 500 μm and 1 mm, 14.1% between 250 μm and 500 μm, 11.2% between 125 μm and 250 μm, 4.2% between 63 μm and 125 μm, and 0.6% < 63 μm. The sands were composed of 1% quartz, 33.1% calcite, and 65.4% aragonite, as determined by X-ray diffraction. The calcite fraction was composed of 2% LMC (2.3 ± 1 mol% MgCO<sub>3</sub>) and 98% HMC (15.2 ± 1 mol% MgCO<sub>3</sub>). Carbonate sands from Heron Island were previously shown to be low in organic carbon content (0.24%) (Wild et al. 2004b).

*Sampling*—During sampling the wind and seas were calm, with minimal cloud cover overhead. Advective chambers were deployed just before midday and sampled every 2 h for 26 h in order to capture an entire diel cycle. Discrete samples were taken from the chambers and water column; the physico-chemical parameters of the water column were also monitored every 20 min with an autonomous probe. A Hydrolab DS5X (Hach Environmental) was deployed 0.2 m from the bottom at the study site to monitor temperature (± 0.5%), PAR (± 5%),

salinity (± 0.5%), and dissolved oxygen (DO; ± 1%) of the water column every 20 min. DO was calibrated to 100% saturated water based on the barometric pressure, and all other sensors were factory calibrated. Discrete water samples were taken every hour from the water column using a 50 mL plastic syringe.

Chambers identical to those described in Glud et al. (2008) and Eyre et al. (2008) were used to measure in situ benthic solute fluxes at three different advection rates. The chamber bottoms extended 15 cm into the sediment and enclosed roughly 4 liters of overlying seawater during the incubations. Advection was induced within the chambers based on the spinning rate, in rotations per minute (RPM), of the acrylic disk within each chamber (diffusive, 40 RPM, and 80 RPM). In order to maintain a homogeneous distribution of solutes within the diffusive chamber it was operated with the disk slowly spinning clockwise for one rotation, then, after a pause, spinning counterclockwise for one rotation and repeating (Glud et al. 2008). The 40 RPM and 80 RPM settings resulted in advective rates of 43 and 213 L m<sup>-2</sup> d<sup>-1</sup>, respectively (Glud et al. 2008). The permeability of the sediment was between  $6.0 \pm 0.7 \times 10^{-11}$  m<sup>-2</sup> and  $1.6 \pm 0.6 \times 10^{-11}$  m<sup>-2</sup> depending on the depth, as measured by Glud et al. (2008). The chambers were deployed over carbonate sands with no visible macrophytes or macrofauna burrows with the lids open for 1 h before being closed at the start of the incubation. Incubations started at 11:40 h on 09 October 2011 and lasted for 26 h. Samples of 150 mL were drawn by syringe every 2 h, with ambient seawater allowed to replace the sample volume. As the seawater composition was similar to the chamber water composition (shown later), no corrections for seawater dilutions were made.

*Sample preparation and analysis*—Both water column and benthic chamber samples were immediately brought back into the laboratory. DO (± 1%) was measured directly following collection using a Hach Luminescent Dissolved Oxygen (LDO®) probe. Samples for nutrients were filtered with a 0.45 μm cellulose acetate filter and frozen at -20°C until analysis, following the methods of Eyre and Ferguson (2005), using a Lachat Flow Injection Analysis system. Samples for total alkalinity (TA) and pH were filtered through a 0.45 μm cellulose acetate filter and stored in an airtight container with no headspace until analysis within 4 h of sampling. pH (± 0.003) was measured using a Metrohm Electrode Plus calibrated to Oakton National Bureau of Standards standards of 4, 7, and 10. To determine TA, Gran titrations were performed using a Metrohm Titrand automatic titrator and pH electrode. Pre-standardized 0.01 mol L<sup>-1</sup> HCl was used as the titrant, which was calibrated against Dickson Certified Reference Material (Batch 111). Alkalinity samples were run twice and the average of the two values was used. During the study the uncertainty of duplicate TA measurements was 0.19% ± 0.17%.

Samples for DIC concentrations (± 1.2%) were 0.7 μm filtered with a Whatman GF/F syringe filter, preserved using 50 μL of saturated HgCl with no headspace, and stored at 4°C. For DIC measurements samples were

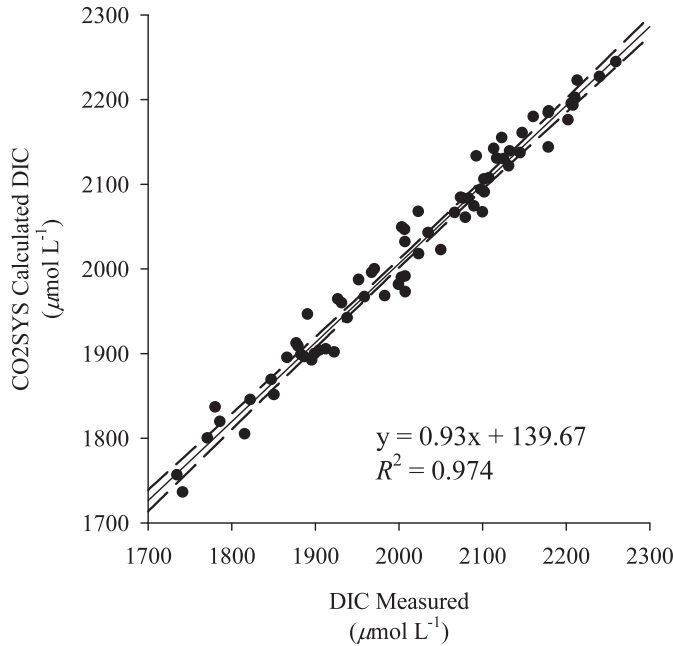


Fig. 1. A regression of measured DIC vs. calculated DIC concentration estimated using the Excel macro CO2SYS. The  $R^2$  and equation for the regression are displayed as well as the 95% confidence intervals (dashed line).

acidified with 5% (v:v) phosphoric acid, and the resulting  $\text{CO}_2$  was analyzed using an Aurora 1030W total organic carbon analyzer (Oakes et al. 2010). DIC concentrations were also estimated with the Excel macro CO<sub>2</sub> System (CO2SYS) (Pierrot et al. 2006) using inputs of TA and pH and the constants from Mehrbach et al. (1973) refit by Dickson and Millero (1987). CO2SYS also generated saturation states ( $\Omega$ ) for calcite and aragonite. A linear regression ( $R^2 = 0.974$ ) of measured and calculated DIC concentrations demonstrated an excellent agreement between the two methods over the concentration range measured during this study (Fig. 1). Measured DIC values were used for all further calculations.

Carbonate alkalinity ( $\text{TA}_C$ ) for each sample was calculated by subtracting the alkalinity, as determined in CO2SYS using TA and pH, contributed by  $\text{B}(\text{OH})_4^-$ ,  $\text{OH}^-$ , and total dissolved phosphorus (TDP) from TA. The contribution to TA from each of the above ions was within the following ranges;  $\text{B}(\text{OH})_4^-$  contributed between 60 and 130  $\mu\text{mol kg}^{-1}$ ,  $\text{OH}^-$  5 to 12  $\mu\text{mol kg}^{-1}$ , and TDP contributed around 1  $\mu\text{mol kg}^{-1}$  for each sample.  $\text{TA}_C$  was also corrected for  $\text{NH}_4^+$  and  $\text{NO}_3^-$ , which represented a minor component to alkalinity ( $\leq 1 \mu\text{mol kg}^{-1}$ ).

**Calculation of rates**—Hourly flux rates of solutes from the sediment were calculated using the following equation:

$$r_x = \frac{\Delta s_x \times h}{\Delta t} \quad (1)$$

where  $\Delta s_x$  is the change in solute concentration (in  $\mu\text{mol L}^{-1}$ ),  $h$  is the average height of water enclosed within the chamber (in meters),  $\Delta t$  is the change in time (in hours), and  $r_x$  is the hourly flux rate of solute  $x$  (in  $\text{mmol m}^{-2} \text{h}^{-1}$ ).

The net daily flux rate of a solute from the sediment was calculated using three separate approaches. The first approach, as typically used by most investigators (Rasheed et al. 2004; Rao et al. 2012), relies on the linear slope of the solute concentration vs. time during both daytime and nighttime hours. The slopes were then converted to  $\text{mmol m}^{-2} \text{h}^{-1}$ , multiplied by either the amount of daylight (13 h) or darkness (11 h), and added together. The second approach used the concentrations at the start and end points of the light and dark periods over an entire diel cycle and calculated fluxes based on the sum of changes between those concentrations (Ferguson et al. 2003; Eyre et al. 2008).

The third approach involved plotting hourly rates against time and integrating the underlying area based on the equation for the area of a trapezoid,

$$i_x = \frac{\Delta t \times (r_{x1} + r_{x2})}{2} \quad (2)$$

where  $r_{x1}$  and  $r_{x2}$  are the hourly flux rates of solute  $x$  during the time interval  $\Delta t$  and  $i_x$  is the integrated flux rate of solute  $x$  (in  $\text{mmol m}^{-2}$ ). The resulting fluxes can then be added up to represent a 24 h time period and are presented as  $\text{mmol m}^{-2} \text{d}^{-1}$ . By dividing  $i_x$  by its associated time interval, the integrated rates can be converted back to hourly integrated rates, which were used for all subsequent analyses. Negative rates designate a flux into the sediment from the water, while a positive rate designates a flux out of the sediment.

Based on reaction stoichiometry, alkalinity can be used to determine the contribution of precipitation and dissolution to the DIC pool by dividing  $\text{TA}_C$  in half. The flux rate of DIC due to respiration and photosynthesis can then be calculated by subtracting half of the  $\text{TA}_C$  flux rate from the overall DIC flux rate, which we term  $\text{DIC}_{\text{TA}_C}$ . However, this assumes that no other reactions (e.g., sulfate reduction) are contributing or consuming alkalinity (see Discussion).

## Results

**Solute concentrations**—PAR measured during the incubations is shown in Fig. 2. Both DO concentrations and pH increased during the daylight hours and decreased at night, with the greatest range in the 80 RPM chamber (Fig. 3). The concentrations of TA and DIC showed the same trend, increasing at night and decreasing in the day, with the greatest range in the 80 RPM chamber. Although both  $\Omega$  of calcite and aragonite varied during the course of the day, neither reached the theoretical dissolution threshold of 1. The range of solute concentration within the chambers, particularly the 40 RPM chamber, was similar to the natural range measured in the water column (Fig. 3).

**Integrated fluxes**—Integrated flux rates ( $i_x$ ) of DO,  $\text{H}^+$ ,  $\text{TA}_C$ , and  $\text{DIC}_{\text{TA}_C}$  showed a distinct diel cycle (Fig. 4). Flux rates of DO and  $\text{DIC}_{\text{TA}_C}$  changed similarly among the three chambers during the daytime (Fig. 4A,C). However, during the night, DO and  $\text{DIC}_{\text{TA}_C}$  showed differing trends. In the 80 RPM chamber, DO rates leveled off for most of the night, while in the diffusive and 40 RPM chamber they increased after 2 h of darkness and moved toward more

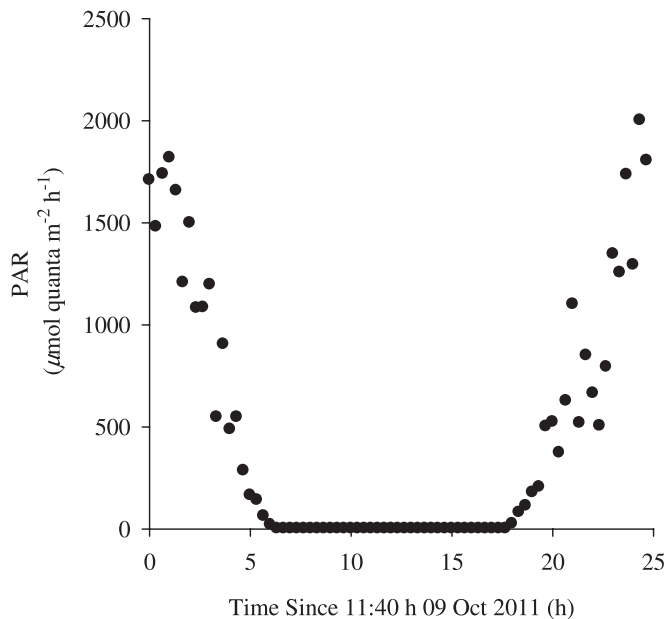


Fig. 2. PAR levels measured over the course of the incubations.

positive values throughout the night.  $\text{DIC}_{\text{TAC}}$  fluxes had similar but opposite trends during the night (Fig. 4C).  $\text{DIC}_{\text{TAC}}$  flux rates from both the 40 and 80 RPM chambers changed sharply from uptake to efflux during first 2 h after sunset and then began to drop during the rest of the night and throughout the day. In the diffusive chamber,  $\text{DIC}_{\text{TAC}}$  fluxes showed a pattern similar to  $\text{TA}_{\text{C}}$  fluxes, increasing to a peak in the middle of the night.  $\text{H}^+$  fluxes showed the highest variation between the different advection rates and steadily increased during the night and decreased during the day (Fig. 4B).

## Discussion

*Chamber artefacts and operation*—A previous study (Glud et al. 2008) from a similar study site using the same chambers and stirring rates showed much less variation between replicates for rates of productivity and respiration than between stirring rates. As such, we used a range of chamber stirring rates but did not perform replication. Although concentrations in the chambers changed dramatically over the diel cycle, which would influence the sediment biogeochemistry, the changes in the diffusive and 40 RPM chambers were similar to those in the water column (Fig. 3). For example, overnight the % DO saturation in the water column decreased to 70%, while it decreased to 97%, 77%, and 33% in the diffusive, 40 RPM, and 80 RPM chambers, respectively. The similarity in concentration changes between the water column and the 40 RPM chamber indicates that the biogeochemical processes in the chambers reflect the natural sediments and that any major changes were unlikely due to incubation artefacts.

There are numerous mechanisms that induce the advection of overlying water into sediments that act on

different spatial and temporal scales (Santos et al. 2012). The advective chambers used in this study were designed to induce advection that is similar to flow- and topography-induced advection [see fig. 1(5) in Santos et al. (2012)], but not necessarily designed to simulate in situ advective rates. The main advantage of using these chambers is that they allow for the manipulation of filtration rates in order to investigate the effects of advective rates on biogeochemical processes. However, the 40 and 80 RPM chambers induced filtration rates of 43 and 213  $\text{L m}^{-2} \text{d}^{-1}$ , respectively, in Heron Island sediments (Glud et al. 2008). These chamber-induced filtration rates are on the same order of magnitude as in situ filtration rates established from artificial ( $264 \text{ L m}^{-2} \text{d}^{-1}$ ) (Wild et al. 2004a) and natural tracer observations ( $\sim 150 \text{ L m}^{-2} \text{d}^{-1}$ ) (Santos et al. 2010) at the same location in Heron Island. As a result of the above issues, and given the fact that the sediment incubations were based on only one diel cycle, net daily flux rates from this study must be interpreted carefully.

*Influence of calculation method on net daily benthic flux rates*—The method used to calculate net daily flux rates can have a significant effect on both the magnitude and direction of the rate. The flux rates generated from the integration and end-point methods were similar in magnitude and direction of the fluxes, while the rates generated from linear regressions tended to be overestimated and in the opposing direction (Table 1). This is probably due to the regression-based method overestimating photosynthesis in the daylight hours when not taking into account the changes in rates caused by fluctuations in PAR (discussed in further detail later). In addition, nighttime respiration rates calculated by integration varied considerably (Fig. 4). This variability in nighttime flux rates would have an effect on net daily rate calculations that would lead to the over- or underestimation of nighttime rates, depending on how the incubations are performed.

Most previous studies in coral reef sands have carried out benthic flux incubations that last on timescales of 4 to 8 h and measure dark respiration by blocking sunlight during the day (Rasheed et al. 2004; Rao et al. 2012) or during early dark hours (Boucher et al. 1998). Shorter incubations increase the potential to drastically under- or overestimate benthic fluxes depending on the time of day at which the incubations are done (Fig. 4). If incubations are performed during early evening hours they have the potential to overestimate nighttime respiration on a daily basis. If incubations are performed during daylight hours by covering the chamber with dark material, respiration rates may be underestimated, as primary production may be inhibited, potentially reducing the amount of labile organic material available for respiration.

When the linear regression approach is used to calculate net daily fluxes the sediments are net autotrophic, but when the integral-based approach is used they are net heterotrophic based both on DIC and DO concentrations (Table 1). Net daily  $\text{TA}_{\text{C}}$  fluxes are also opposite depending on the calculation method employed. When the regression rate is used, alkalinity is fluxed into the sediments (i.e., net precipitation is occurring). However, when the integral-

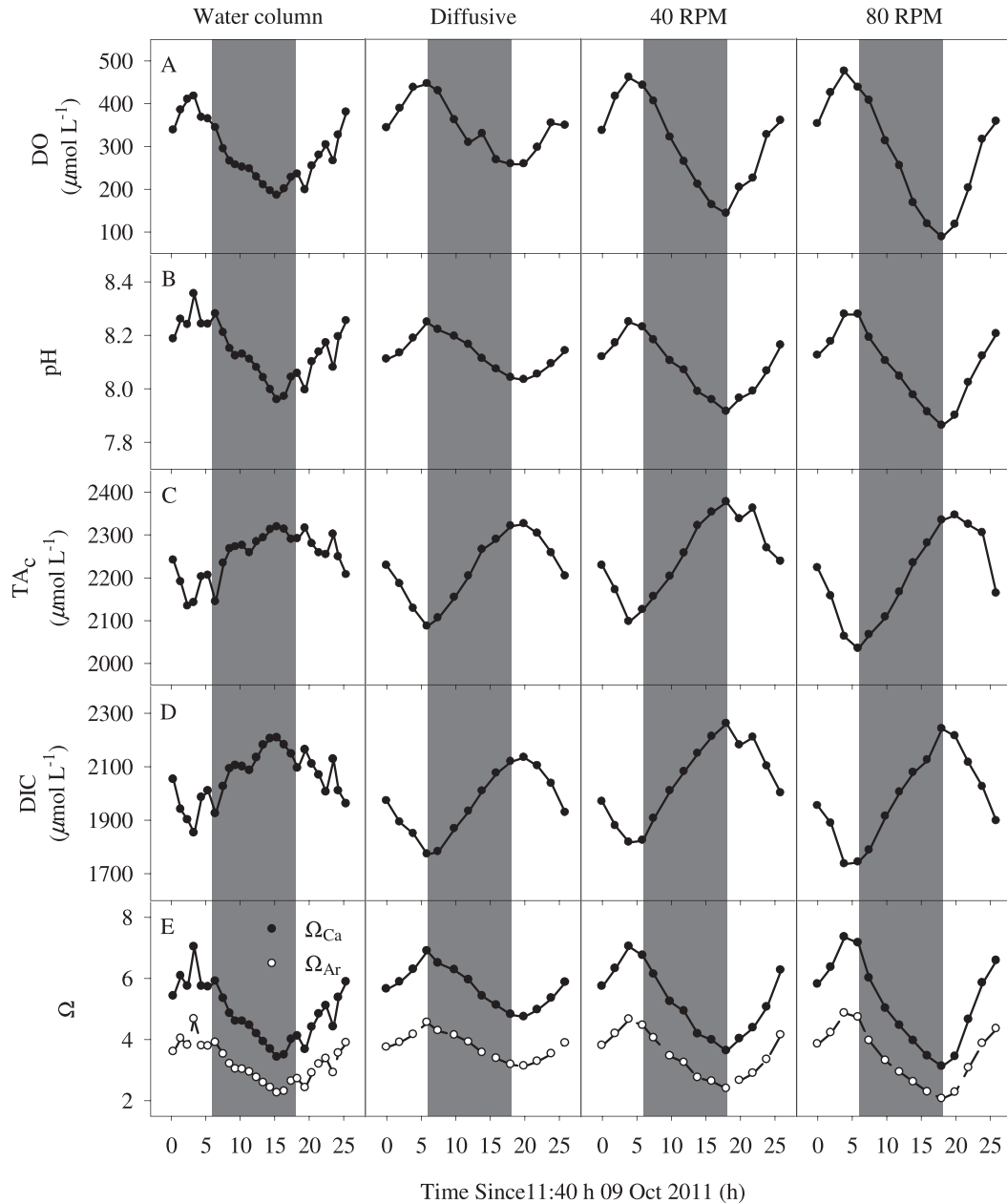


Fig. 3. (A) DO, (B) pH, (C)  $TA_C$ , (D) DIC, and (E) saturation state of calcite ( $\Omega_{Ca}$ ) (closed circles) and aragonite  $\Omega_{Ar}$  (open circles) in the water column and the three benthic chambers over the course of the incubations. The dark gray bars indicate nighttime hours. The incubations started on 09 October 2011 at 11:40 h.

based approach is used net dissolution of the sediments is occurring. These results emphasize the importance of measuring flux rates over the course of an entire diel cycle. This complete reversal in the dynamics of benthic ecosystems can have a large influence on community-level models and our understanding of their biogeochemistry. The diel variability of respiration, photosynthesis, and carbonate precipitation and dissolution needs to be taken into account when calculating net flux rates.

However, if incubations are performed over the course of an entire diel cycle and the end-point method (Ferguson et al. 2003; Glud et al. 2008) is used to calculate flux rates, there is good agreement with the integral-based method (Table 1).

Even though the end-point method yielded net flux rates that were similar to those associated with the integral-based method there were still discrepancies between some of the flux rates (Table 1). This may be due to the fact that the end-point method does not take into account the small changes in hourly flux rates that occur over a diel cycle (Fig. 4). As a result of the more detailed information provided by the integral-based approach, net flux rates used in the “Discussion” were calculated by integration.

*Biological and geochemical carbon cycling based on DIC and  $TA_C$  regressions*—The proportion of DIC flux due to biological (respiration and photosynthesis, also referred to

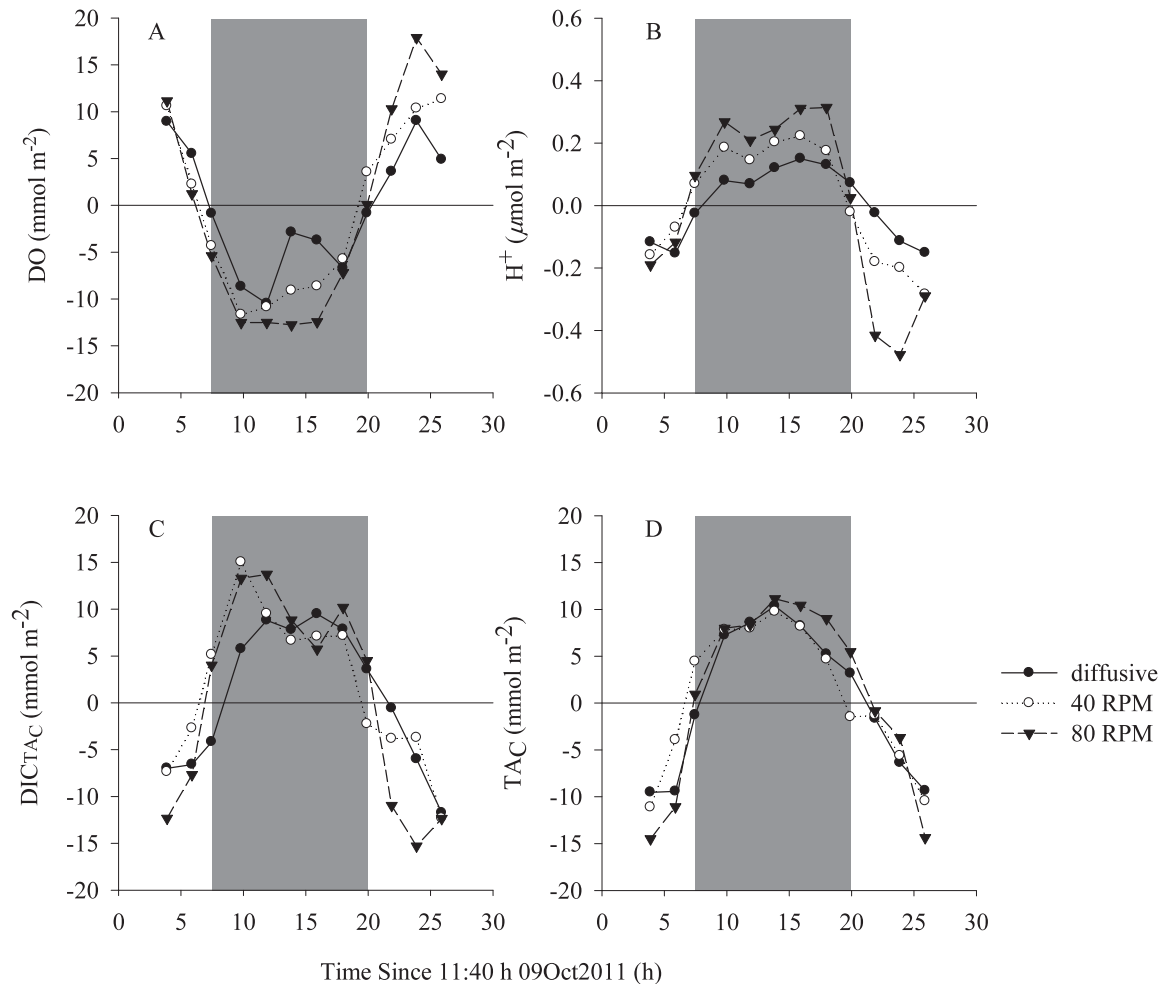


Fig. 4. Integrated fluxes of (A) DO, (B) H<sup>+</sup>, (C) DIC<sub>TAc</sub>, and (D) TAc from the diffusive, 40 RPM, and 80 RPM chambers plotted against the time since the start of the incubation. Dark gray bars indicate nighttime hours.

as organic metabolism by others) and geochemical (carbonate precipitation and dissolution, also referred to as inorganic metabolism by others) processes can be determined from the slope of DIC vs. TAc by accounting for the portion of DIC flux due to carbonate precipitation and dissolution (Gattuso et al. 1996). As the stirring rate increases, the ratio of DIC flux due to biological processes to the DIC flux due to geochemical processes increases from 1.99 to 2.40 (Fig. 5; Table 2). These results are consistent with the stimulation of oxidative respiration by advection in carbonate sands (Glud et al. 2008). The increase in this ratio may be due to the stimulation of photosynthesis during the daylight hours at higher

advection rates (see Fig. 4A) and subsequent release of more organic carbon that is available for respiration (Cook and Røy 2006). Whole-community coral reef fluxes have been shown to have biological to geochemical ratios of DIC fluxes that range from 3 to 6 (Frankignoulle et al. 1996; Gattuso et al. 1996). The ratio of concentrations in the water column was close to the bottom end of that range, at 2.83 (Fig. 6; Table 2). Because carbonate sediments contain a large pool of inorganic carbon it is not surprising that the DIC flux rates from the sediments have a lower biological to geochemical ratio than those of whole-reef communities, which are influenced by both benthic and pelagic processes.

Table 1. Net daily flux rates of TAc, DIC<sub>TAc</sub>, DO, and H<sup>+</sup> calculated using the integral (Int)-, end-point (EP)-, and regression (Reg)-based approaches. All values are in mmol m<sup>-2</sup> d<sup>-1</sup>, except for H<sup>+</sup> fluxes, which are in μmol m<sup>-2</sup> d<sup>-1</sup>.

Chamber	TAc			DIC <sub>TAc</sub>			DO			H <sup>+</sup>		
	Int	EP	Reg	Int	EP	Reg	Int	EP	Reg	Int	EP	Reg
Diffusive	5.13	5.58	-14.03	7.19	9.28	-9.67	-2.29	2.05	16.37	0.038	0.057	-0.200
40 RPM	8.84	6.82	-17.37	18.34	18.80	-2.88	-5.24	-1.62	17.95	0.088	0.166	-0.293
80 RPM	8.78	14.66	-31.27	1.64	5.43	-2.31	-8.17	-6.59	24.59	-0.022	0.010	-0.486

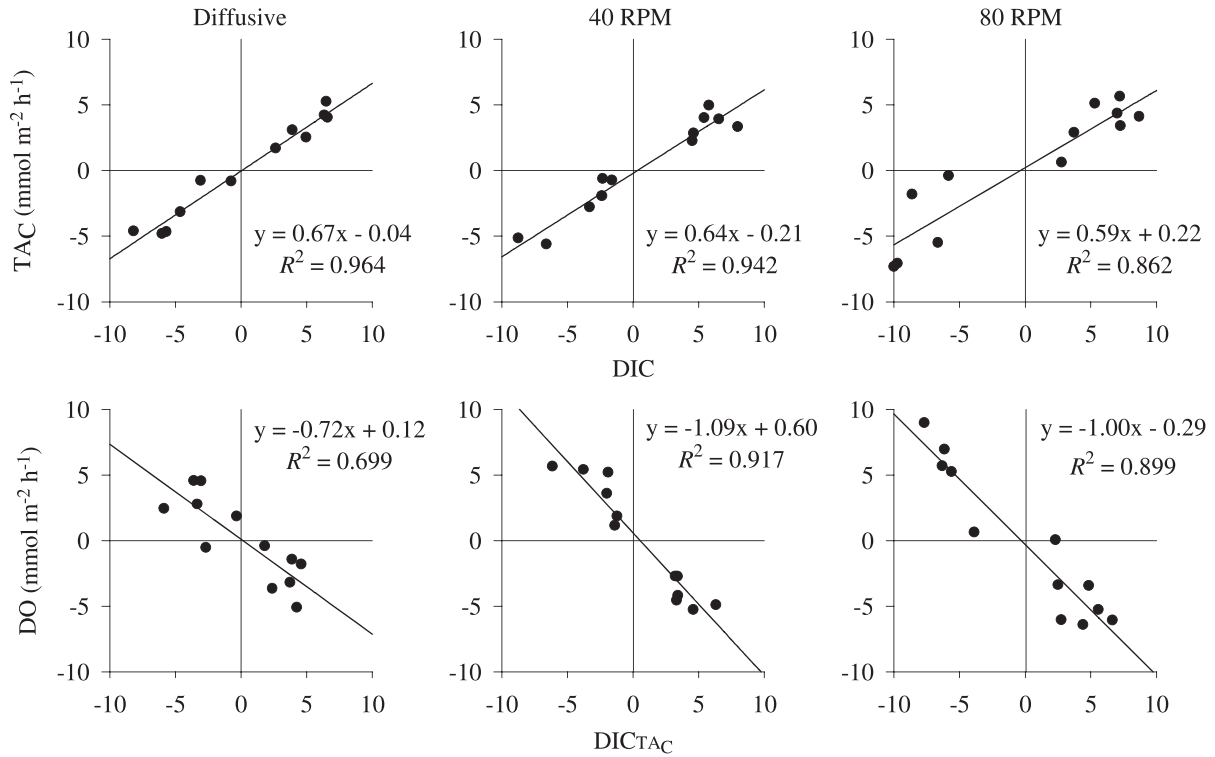


Fig. 5. Regressions of TA<sub>C</sub> vs. DIC and DO vs. DIC<sub>TA<sub>C</sub></sub> fluxes from all three chambers.

Another process that could potentially affect sediment alkalinity fluxes is the uncoupling of sulfate reduction and sulfide oxidation (Ku et al. 1999). Regressions of DIC<sub>TA<sub>C</sub></sub> vs. DO fluxes from the 40 RPM and 80 RPM chambers (i.e., when advection is induced) have slopes very close to  $-1$ , indicating that once the DIC flux rates are corrected for the precipitation and dissolution of carbonates the two methods of measuring respiration and photosynthesis agree closely (Fig. 5). If there were an uncoupling of sulfate reduction and sulfide oxidation in anoxic zones (and subsequent increase in alkalinity), we would expect to see an increase in DIC<sub>TA<sub>C</sub></sub> unaccounted for by a decrease in DO (Eyre and Ferguson 2002), which is not observed in the advective chambers. This lends support not only to the two methods used to calculate photosynthesis and respiration rates but also to the majority of alkalinity changes being accounted for by the precipitation and dissolution of carbonate minerals. In addition, sulfate concentrations have been shown to be conservative in carbonate sediments to depths at which the advective cycling of pore waters is

occurring, indicating no net flux of alkalinity due to these processes (Burdige and Zimmerman 2002).

*Effects of  $\Omega_{Ar}$  on benthic fluxes of alkalinity*—When graphed against  $\Omega_{Ar}$ , alkalinity fluxes follow a distinct diel hysteretic pattern (Fig. 7). Interestingly, TA<sub>C</sub> flux does not follow a trend consistent with the  $\Omega_{Ar}$  of the water column being the main driver of carbonate precipitation and dissolution. Instead, carbonate precipitation and dissolution is linearly correlated to the rates of photosynthesis and respiration occurring over the same time period (Fig. 8). It seems that even though respiration decreases  $\Omega_{Ar}$  consistently throughout the night (Fig. 3), dissolution is more closely linked to the amount of respiration occurring than to the bulk  $\Omega_{Ar}$  of the overlying water. This is consistent with the hypothesis that DIC within the microenvironments of carbonate sediment grains is intimately linked to the precipitation and dissolution of carbonate minerals (Henrich and Wefer 1986; Freiwald 1995).

Table 2. The  $R^2$ , y-intercept ( $y_0$ ), and slope values from the regression analysis of DIC vs. TA<sub>C</sub> fluxes shown in Fig. 5. Percent precipitation was determined by dividing the slope by 2 and multiplying that value by 100. The ratios of biological (bio) to geochemical (geo) DIC fluxes were calculated from the slope.

Chamber	$R^2$	$y_0$	Slope	% Geochemical	DIC bio : geo
Diffusive	0.964	-0.040	0.669	33.5	1.99
40 RPM	0.942	-0.207	0.637	31.9	2.14
80 RPM	0.862	0.219	0.589	29.5	2.40
Water column	0.921	1175.40	0.522	26.1	2.83

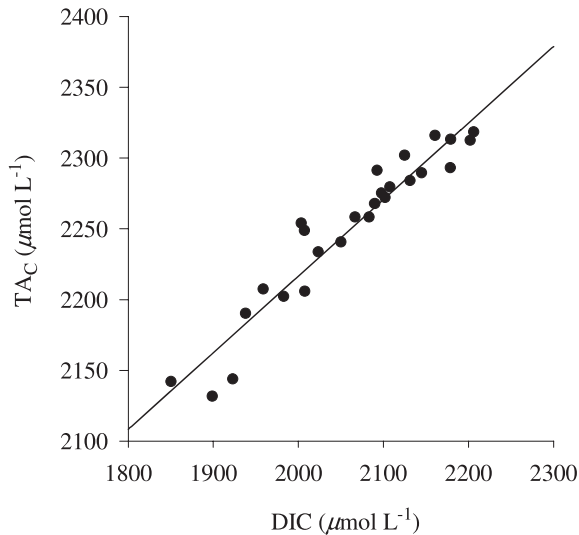


Fig. 6. Regression of  $TA_C$  vs. DIC concentrations from the water column.

These results have implications for using the  $\Omega_{Ar}$  of seawater as an overall indicator of carbonate precipitation and dissolution in sediments. Whole-system calcification is often assumed to be linearly dependent on  $\Omega_{Ar}$  (see fig. 6 in Shamberger et al. [2011]). However, our results show that the processes occurring within permeable carbonate sediments make this interpretation much more complex (Fig. 7). Shamberger et al. (2011) used daily flux rates, which would obscure any hysteretic pattern, as evidenced by hourly flux rates. In large-scale models (Morse et al. 2006) using the  $\Omega_{Ar}$  of overlying seawater to estimate the dynamics of carbonate dissolution in the sediments may misinterpret what is occurring. If respiration drives the dissolution of carbonates within microenvironments, pore

waters, and especially the overlying waters, do not need to reach a  $\Omega < 1$  of metastable minerals for dissolution to occur. In fact, Andersson et al. (2007) found that sediment dissolution rates in Devil's Hole, Bermuda, were similar to those reported throughout the literature despite the fact that the overlying water at their study sites had a much lower  $\Omega_{Ar}$ . Even if pore waters have high  $\Omega_{Ar}$ , microenvironments may promote the dissolution of carbonates and the export of alkalinity into the water column.

*Effects of PAR on integrated flux rates*—Integrated hourly fluxes of DO and DIC were clearly related to the average PAR measured during the same time interval (Fig. 9). By plotting DO and DIC fluxes against PAR, photosynthesis–irradiance (P-I) curves can be generated that allow for the modeling of production based on the amount of PAR received. The benthic  $DIC_{TA_C}$  and DO fluxes show trends consistent with P-I curves of whole-ecosystem studies (Gattuso et al. 1996). The DO fluxes fit well to logarithmic curves, with all of the  $R^2$  values above 0.795 (Fig. 9). Based on the logarithmic fit, the maximal hourly fluxes of DO increased with advection rates from 3.13 to 4.85 to 6.19  $mmol\ m^{-2}\ h^{-1}$  in the diffusive, 40 RPM, and 80 RPM chambers, respectively. This is consistent with the results of other studies (Cook and Røy 2006; Glud et al. 2008), which show the stimulation of benthic primary productivity with increased advection. DIC fluxes were similarly stimulated by PAR, but in both the diffusive and 40 RPM chambers a maximal was not reached, so linear regressions were used. At 80 RPM a logarithmic function fit the data with an  $R^2$  of 0.848 and a maximal daytime flux rate of  $-5.39\ mmol\ m^{-2}\ h^{-1}$  (Fig. 9).

No distinct P-I-like trend was observed for the  $TA_C$  flux vs. PAR plot (Fig. 10). Instead, the magnitude of the rates

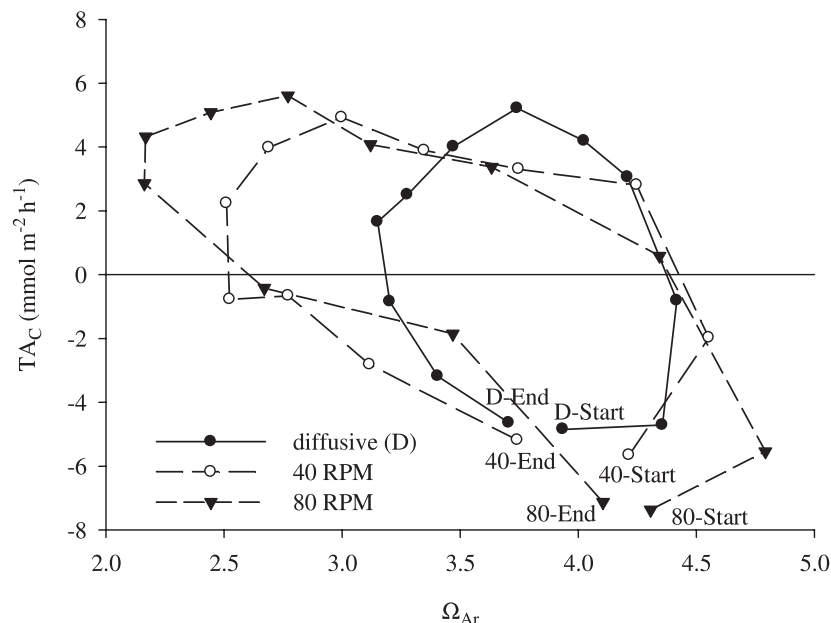


Fig. 7. Carbonate alkalinity fluxes ( $TA_C$ ) plotted against the saturation state of the overlying water during the incubations. The start and end points are shown, and the flux rates are plotted from the beginning to the end of the incubations.

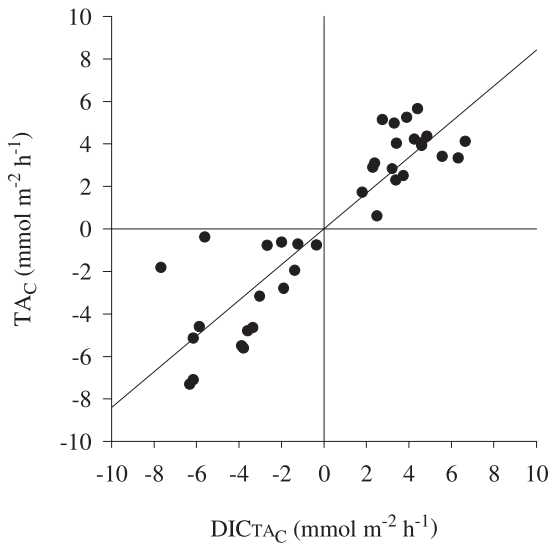


Fig. 8.  $TA_C$  fluxes plotted against  $DIC_{TA_C}$  fluxes from all of the chamber incubations.

was highly influenced by the time of day, showing a hysteretic trend. The influx of alkalinity into the sediments (precipitation) increased with higher PAR, but the rates recorded in the morning were lower than those time intervals receiving similar PAR levels in the afternoon. This is most likely due to the lowering of the carbonate mineral saturation state in the pore waters overnight as a result of respiration (Fig. 3). As the saturation state increased during the day as a result of benthic photosynthesis, so too did the rates of precipitation. These observations are consistent with reports (Goreau 1959; Pearse and Muscatine 1971) of photosynthesis having a stimulating effect on calcification in corals.

These results showed not only that solute fluxes over a 24 h period were highly dependent on the amount of PAR reaching the benthos but also that fluxes were highly variable throughout the night (Figs. 3,6,7). This observation supports our earlier suggestion that shorter incubations (Rasheed et al. 2004; Rao et al. 2012) may not accurately reflect the changes in respiration occurring

throughout the night. The results also imply (especially in the case of  $TA_C$  fluxes) that performing dark incubations during the daylight hours and extrapolating those rates to nighttime hours can grossly over- or underestimate rates based on the starting conditions within the incubation.

For example, Rao et al. (2012) performed similar incubations to ours but covered the chambers with dark material and performed both light and dark incubations for 5 h starting at midday. Using the slope-based method to calculate net flux rates, combined with their experimental methodology, would result in artificially lowered dark alkalinity efflux rates due to the time of day during which the incubations were performed (Fig. 4). In sediments similar to ours, Rao et al. (2012) generally found lower dark ( $1.0$  to  $2.1$   $mmol\ m^{-2}\ h^{-1}$ ) and net daily ( $-5.32$  to  $8.22$   $mmol\ m^{-2}\ d^{-1}$ ) flux rates of alkalinity than those described here. In addition, the net daily release of alkalinity decreased with increasing advection rate, with the sediments becoming net sinks at the highest advection rates (Rao et al. 2012). This supports the idea that diel variability should be taken into account when calculating net daily flux rates, as there is a large potential for methodology to greatly influence the magnitude and direction of the rate. Because the amount of PAR reaching the sediments greatly influenced their biogeochemistry, it may also be important to measure these cycles over daily and seasonal timescales that represent natural variability in PAR.

*Interaction of advection and carbonate precipitation and dissolution*—Pore-water advection has been shown to have a large effect on the rates of photosynthesis and respiration occurring in permeable sediments (Janssen et al. 2005; Glud et al. 2008). Our experiment adds to previous work by demonstrating the advective stimulation of carbonate dissolution (Table 1; Fig. 4). Interestingly, the rates of photosynthesis and respiration are stimulated equally by advection. In the diffusive chamber the maximum rate of photosynthesis was  $5.83$   $mmol\ C\ m^{-2}\ h^{-1}$ , and the maximum rate of respiration was  $4.63$   $mmol\ C\ m^{-2}\ h^{-1}$ . The maximal hourly photosynthetic rate within the 80 RPM chamber was  $7.64$   $mmol\ C\ m^{-2}\ h^{-1}$ , while the maximum

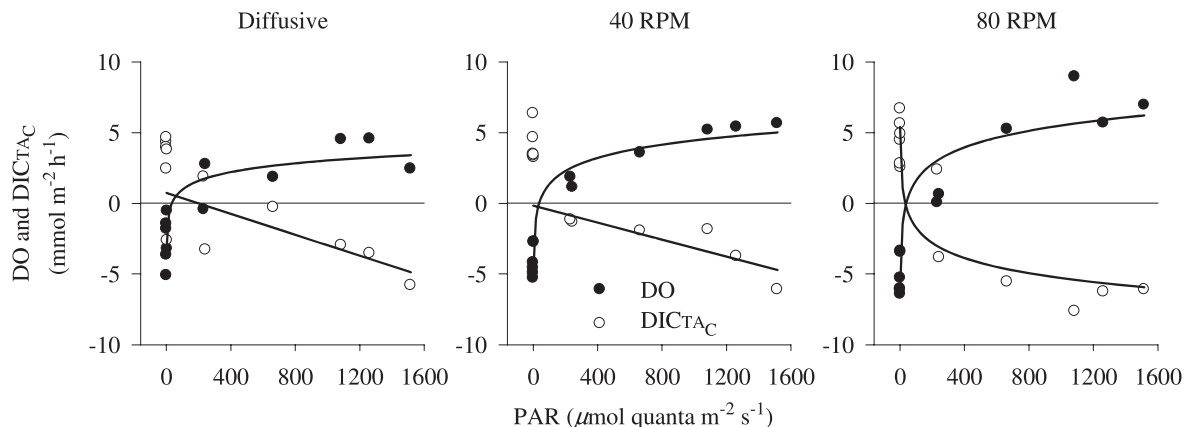


Fig. 9. DO and  $DIC_{TA_C}$  fluxes plotted against the average PAR measurements made during the same time period in which the flux was measured. Regressions are displayed as explained in the text.

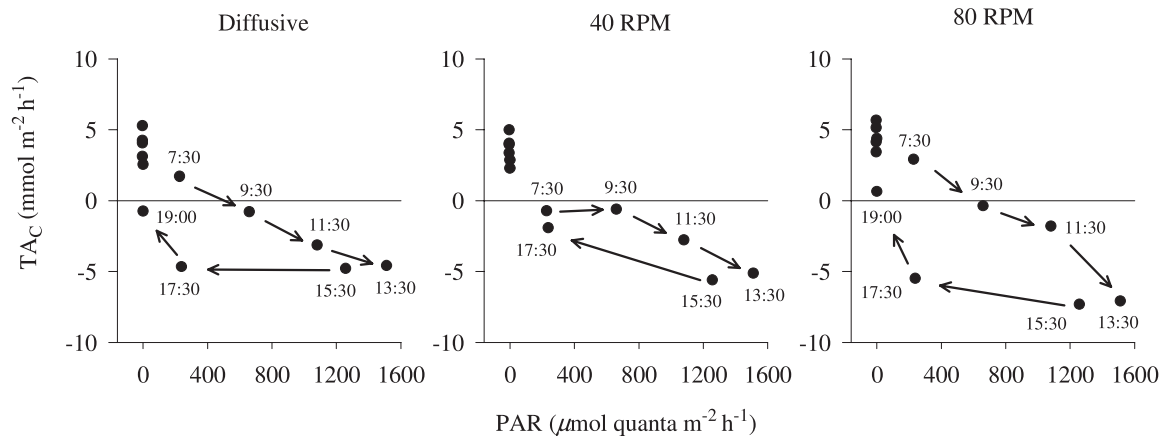


Fig. 10.  $TA_C$  fluxes plotted against the average PAR measurements made during the same time period in which the flux was measured. The start time for each flux measurement is written next to the data point, with arrows showing the historical trends described in the text.

nighttime respiration rate was  $6.69 \text{ mmol C m}^{-2} \text{ h}^{-1}$ . Precipitation is stimulated by advection during the day, with maximal hourly  $TA_C$  flux rates of  $-4.83$ ,  $-5.65$ , and  $-7.36 \text{ mmol m}^{-2} \text{ h}^{-1}$  in the diffusive, 40 RPM, and 80 RPM chambers, respectively. Maximal efflux rates of  $TA_C$  during the night (dissolution) also increase with stirring rates from  $5.21$  to  $5.65 \text{ mmol m}^{-2} \text{ h}^{-1}$  between the diffusive and 80 RPM chambers. The maximum alkalinity efflux rates from this study are roughly five times higher than previously reported, non-advective rates from similar carbonate environments (Table 3). On a daily basis alkalinity is fluxed out of the sediments and into the water column, with similar rates in the 40 RPM and 80 RPM chambers (Table 1).

There are a few potential reasons why advection stimulates the release of alkalinity from sediments. Firstly, advection stimulates respiration (Glud et al. 2008), which would induce  $TA_C$  efflux as a result of the tight coupling of respiration and carbonate dissolution (Fig. 8). However, one interesting aspect of advective stimulation is that there is a balance between flux rates at the higher advection rates because counteracting processes (photosynthesis and

respiration) may be stimulated in a similar manner. This can have a large effect on daily alkalinity fluxes, which are highly dependent on those processes. This complex interaction between the advective stimulation of photosynthesis and respiration may drive the advective stimulation of carbonate dissolution on a daily basis. Secondly, advection also increases the volume of sediment that is in contact with water being delivered to the overlying water column, which could lead to higher dissolution rates, although this is reflected in the enhanced respiration. Thirdly, the water being advected into the sediments introduces oxygen to greater depths, which would decrease sulfate reduction and the associated production of alkalinity (Ku et al. 1999; Morse et al. 2006). This reduction in alkalinity may lower the  $\Omega_{Ar}$  of the pore water, subsequently promoting the dissolution of carbonates. Figure 8 implies that enhanced respiration is probably the main driver of increasing carbonate dissolution associated with increasing advection, although some of the scatter in Fig. 8 may be due to sulfate reduction. Further work is required to unravel the complex interactions between advection,

Table 3. Hourly alkalinity efflux rates from carbonate sands. “Method” refers to the method used to calculate alkalinity fluxes.

Location	Bottom type	Alkalinity flux ( $\text{mmol m}^{-2} \text{ h}^{-1}$ )	Method	Source
Bahamas	Oolitic carbonate sands	0.008–0.08	Diffusive flux estimated from pore-water solute concentration	Burdige and Zimmerman 2002
Bermuda	Carbonate sediments	0.4–1.6	Alkalinity excess and vertical eddy diffusion	Andersson et al. 2007
Bermuda	Carbonate sediments	0.6	Bell jar incubation	Balzer and Wefer 1981
Biosphere 2	Carbonate sediments	0.4	Mesocosm incubation	Langdon et al. 2000
Florida	Carbonate sand bottom	0.06	Chamber incubation	Yates and Halley 2003
Hawaii	Carbonate sand bottom	0.06	Chamber incubation	Yates and Halley 2003
Heron Island	Carbonate sediments	0.5–5.6	Advective chamber incubation over complete diel cycle	This study
Heron Island	Carbonate sediments	1.0–2.1	Light and dark advective chamber incubations	Rao et al. 2012
Mesocosm	Carbonate sand	1.6	Mesocosm incubation	Leclercq et al. 2002
Moorea	Carbonate sand bottom	1.6	Chamber incubation	Boucher et al. 1998

Table 4. Results of community flux rates calculated at low tides during the incubations. An average depth of 1.7 m was assumed for the lagoon. Fluxes 1 and 3 were during daylight hours, and flux 2 was at night. The flux rates from the chambers were calculated during the same time interval as the community flux rates. All rates are in  $\text{mmol m}^{-2} \text{h}^{-1}$ .

Sample	DO	TA <sub>C</sub>	DIC	DIC <sub>TA<sub>C</sub></sub>
Community-1	45.20	-109.50	-60.76	-79.12
Diffusive-1	3.64	-4.77	-5.81	-3.43
40 RPM-1	3.25	-3.82	-4.46	-2.55
80 RPM-1	3.14	-6.45	-8.28	-5.06
Community-2	-24.60	42.77	21.33	32.11
Diffusive-2	-2.52	3.25	5.82	4.63
40 RPM-2	-3.48	3.12	5.00	3.46
80 RPM-2	-4.76	4.71	6.19	2.79
Community-3	48.43	-80.03	-48.20	-55.93
Diffusive-3	2.42	-4.64	-8.15	-5.83
40 RPM-3	5.63	-5.18	-8.70	-6.11
80 RPM-3	6.94	-7.14	-9.69	-6.12

benthic respiration and production, and carbonate dissolution in permeable sediments.

*Contribution of sediments to community-scale processes*—Since low tides isolate the Heron Island lagoon from mixing with open ocean water, whole-community fluxes for the lagoon can be estimated based on solute concentration changes during those times (Santos et al. 2011). Our community rates calculated during low tides agree well with those of other studies (Frankignoulle et al. 1996; Gattuso et al. 1996) measuring community rates of photosynthesis and respiration on coral reefs, which report a range of community respiration and photosynthesis from 31 to 52  $\text{mmol C m}^{-2} \text{h}^{-1}$  (Table 4). Hourly fluxes from the sediments during the same time period of the low tides were compared to whole-community fluxes obtained for the three low tides covered by our water column time series (Table 4). According to whole-community estimates from our data, sediments contribute 3% to 14% of community photosynthesis and 3% to 9% of precipitation during the day. At night sediments contribute 9% to 19% of community respiration and 7% to 11% of community dissolution.

Depending on the rate of advection, the dissolution of carbonate minerals fluxes 5.13 to 8.84  $\text{mmol m}^{-2} \text{d}^{-1}$  of alkalinity into the water column from the sediments (Table 1). Because sediments make up roughly 85% of the 26.4  $\text{km}^2$  reef flat (Glud et al. 2008), they contribute a total of 115 to 199  $\text{kmol d}^{-1}$  of carbonate alkalinity into the system. If we assume the coral community calcification rate at Heron Island to be 100  $\text{mmol CaCO}_3 \text{ m}^{-2} \text{d}^{-1}$  (Nakamura and Nakamori 2009) and the remaining 15% of the reef flat to be covered by corals, then the uptake of carbonate alkalinity by corals is estimated as 792  $\text{kmol d}^{-1}$ . From a mass-balance standpoint this means that on a daily basis the sediments can supply 14% to 25% of the carbonate alkalinity consumed by corals within the Heron Island reef flat. It is unresolved whether corals grow at the expense of sediment dissolution, as opposed to the commonly held notion that corals supply carbonate to

the sediment pool, although there is probably a complex cycling that occurs between these two pools of carbonate minerals.

*Potential implications for ocean acidification*—By using a simple calculation similar to the one above we can estimate the addition of  $\text{H}^+$  ions into the system based on rates of ocean acidification. A high-end estimate of pH change is  $-0.002 \text{ pH yr}^{-1}$ , or  $0.0231 \text{ nmol H}^+ \text{ L}^{-1} \text{ yr}^{-1}$  (Gattuso et al. 2011). If we assume an average depth of 1.7 m, there is an increase in  $\text{H}^+$  concentration of  $0.001 \text{ kmol yr}^{-1}$  within the Heron Island reef flat due to ocean acidification. The amount of alkalinity put into the system on a yearly basis from the sediments is estimated as 41,975 to 72,635  $\text{kmol yr}^{-1}$ , orders of magnitude greater than a decrease caused by ocean acidification. While much of the alkalinity produced by sediments will likely be consumed by corals or exported offshore, this simple estimate illustrates the need to consider carbonate sands as an important source of alkalinity.

Previous models relying on diffusive benthic fluxes indicate that sediments in shallow waters can buffer only a minor fraction of anthropogenic  $\text{CO}_2$  inputs (Andersson et al. 2007). Our field observations demonstrate that pore-water advection may enhance the buffering capacity of shallow water sediments against ocean acidification on a local scale, although local hydrodynamics, the ability of a system to accumulate alkalinity, and the concurrent fluxes of  $\text{CO}_2$  with TA will be important (i.e., sediments are unlikely to completely offset the effect of OA on ecological time scales [Andersson et al. 2007]). Also, the magnitude of this buffering capacity is highly dependent on the exact mineralogy, especially the amount of HMCs, of the sediments undergoing dissolution (Morse and Arvidson 2002). Most importantly, because much of the tropical continental shelf is covered by permeable carbonate sediments (Milliman and Droxler 1996), and because permeable sands filter the entire ocean volume on a timescale of about 3000 yr (Santos et al. 2012) and light reaches a large proportion of these shelves (Gattuso et al. 2006), our findings may be applicable to broader areas. Resolving the contribution of pore-water advection in carbonate sands to the global alkalinity budget is important to refining ocean acidification models.

#### Acknowledgments

We thank the staff of the Heron Island Research Station for their invaluable support during our investigations and the staff of the Centre for Coastal Biogeochemistry at Southern Cross University for their assistance in analyzing samples. We also thank the reviewers for their comments on the manuscript. This project was supported by an Australian Research Council Discovery grant awarded to B.D.E. and I.R.S. (DP110103638).

#### References

- ANDERSSON, A., N. BATES, AND F. MACKENZIE. 2007. Dissolution of carbonate sediments under rising  $\text{PCO}_2$  and ocean acidification: Observations from Devil's Hole, Bermuda. *Aquat. Geochem.* **13**: 237–264, doi:10.1007/s10498-007-9018-8

- ANDERSSON, A. J., F. T. MACKENZIE, AND J. P. GATTUSO. 2011. Effects of ocean acidification on benthic processes, organisms, and ecosystems, p. 122–153. *In* J. P. Gattuso and L. Hansson [eds.], *Ocean acidification*. Oxford Univ. Press.
- , ———, AND A. LERMAN. 2005. Coastal ocean and carbonate systems in the high CO<sub>2</sub> world of the Anthropocene. *Am. J. Sci.* **305**: 875–918.
- BALZER, W., AND G. WEFER. 1981. Dissolution of carbonate minerals in a subtropical shallow marine environment. *Mar. Chem.* **10**: 545–558, doi:10.1016/0304-4203(81)90007-4
- BOUCHER, G., J. CLAVIER, C. HILY, AND J. P. GATTUSO. 1998. Contribution of soft-bottoms to the community metabolism (primary production and calcification) of a barrier reef flat (Moorea, French Polynesia). *J. Exp. Mar. Biol. Ecol.* **225**: 269–283, doi:10.1016/S0022-0981(97)00227-X
- BURDIGE, D. J., AND R. C. ZIMMERMAN. 2002. Impact of sea grass density on carbonate dissolution in Bahamian sediments. *Limnol. Oceanogr.* **47**: 1751–1763, doi:10.4319/lo.2002.47.6.1751
- CLAVIER, J., L. CHAUVAUD, P. CUET, C. ESBELIN, P. FROUIN, D. TADDEI, AND G. THOUZEAU. 2008. Diel variation of benthic respiration in a coral reef sediment (Reunion Island, Indian Ocean). *Estuar. Coast. Shelf Sci.* **76**: 369–377, doi:10.1016/j.ecss.2007.07.028
- COOK, P. L. M., AND H. RØY. 2006. Advective relief of CO<sub>2</sub> limitation in microphytobenthos in highly productive sandy sediments. *Limnol. Oceanogr.* **51**: 1594–1601, doi:10.4319/lo.2006.51.4.1594
- DE'ATH, G., J. M. LOUGH, AND K. E. FABRICIUS. 2009. Declining coral calcification on the Great Barrier Reef. *Science* **323**: 116–119, doi:10.1126/science.1165283
- DICKSON, A., AND F. MILLERO. 1987. A comparison of the equilibrium constants for the dissociation of carbonic acid in seawater media. *Deep-Sea Res.* **34**: 1733–1743.
- EYRE, B. D., AND A. J. P. FERGUSON. 2002. Comparison of carbon production and decomposition, benthic nutrient fluxes and denitrification in seagrass, phytoplankton, benthic microalgae and macroalgae-dominated warm-temperate Australian lagoons. *Mar. Ecol. Prog. Ser.* **229**: 43–59, doi:10.3354/meps229043
- , AND ———. 2005. Benthic metabolism and nitrogen cycling in a subtropical east Australian estuary (Brunswick): Temporal variability and controlling factors. *Limnol. Oceanogr.* **50**: 81–96, doi:10.4319/lo.2005.50.1.0081
- , R. N. GLUD, AND N. PATTEN. 2008. Mass coral spawning: A natural large-scale nutrient addition experiment. *Limnol. Oceanogr.* **53**: 997–1013, doi:10.4319/lo.2008.53.3.0997
- FERGUSON, A. J. P., B. D. EYRE, AND J. M. GAY. 2003. Organic matter and benthic metabolism in euphotic sediments along shallow sub-tropical estuaries, northern New South Wales, Australia. *Aquat. Microb. Ecol.* **33**: 137–154, doi:10.3354/ame033137
- FRANKIGNOULLE, M., J. P. GATTUSO, R. BIONDO, I. BOURGE, G. COPIN-MONTÉGUT, AND M. PICHON. 1996. Carbon fluxes in coral reefs. II. Eulerian study of inorganic carbon dynamics and measurement of air-sea CO<sub>2</sub> exchanges. *Mar. Ecol. Prog. Ser.* **145**: 123–132, doi:10.3354/meps145123
- FREIWALD, A. 1995. Bacteria-induced carbonate degradation: A taphonomic case study of *Cibicides lobatulus* from a high-boreal carbonate setting. *Palaios* **10**: 337–346, doi:10.2307/3515159
- GATTUSO, J., M. PICHON, B. DELESALLE, C. CANON, AND M. FRANKIGNOULLE. 1996. Carbon fluxes in coral reefs. I. Lagrangian measurement of community metabolism and resulting air-sea CO<sub>2</sub> disequilibrium. *MEPS* **145**: 109–121, doi:10.3354/meps145109
- GATTUSO, J. P., J. BIJMA, M. GEGHLEN, U. REIBESSELL, AND C. TURLEY. 2011. Ocean acidification: Knowns, unknowns and perspectives, p. 291–311. *In* J. P. Gattuso and L. Hansson [eds.], *Ocean acidification*. Oxford Univ. Press.
- , B. GENTILI, C. DUARTE, J. A. KLEYPAS, J. J. MIDDELBURG, AND D. ANTOINE. 2006. Light availability in the coastal ocean: Impact on the distribution of benthic photosynthetic organisms and their contribution to primary production. *Biogeosciences* **3**: 489–513, doi:10.5194/bg-3-489-2006
- GLUD, R. N., B. D. EYRE, AND N. PATTEN. 2008. Biogeochemical responses to mass coral spawning at the Great Barrier Reef: Effects on respiration and primary production. *Limnol. Oceanogr.* **53**: 1014–1024, doi:10.4319/lo.2008.53.3.1014
- GOREAU, T. F. 1959. The physiology of skeleton formation in corals. I. A method for measuring the rate of calcium deposition by corals under different conditions. *Biol. Bull.* **116**: 59–75, doi:10.2307/1539156
- HENRICH, R., AND G. WEFER. 1986. Dissolution of biogenic carbonates: Effects of skeletal structure. *Mar. Geol.* **71**: 341–362, doi:10.1016/0025-3227(86)90077-0
- HOEGH-GULDBERG, O., AND OTHERS. 2007. Coral reefs under rapid climate change and ocean acidification. *Science* **318**: 1737–1742, doi:10.1126/science.1152509
- JANSSEN, F., M. HUETTEL, AND U. WITTE. 2005. Pore-water advection and solute fluxes in permeable marine sediments (II): Benthic respiration at three sandy sites with different permeabilities (German Bight, North Sea). *Limnol. Oceanogr.* **50**: 779–792, doi:10.4319/lo.2005.50.3.0779
- KU, T. C. W., L. M. WALTER, M. L. COLEMAN, R. E. BLAKE, AND A. M. MARTINI. 1999. Coupling between sulfur recycling and syndepositional carbonate dissolution: Evidence from oxygen and sulfur isotope composition of pore water sulfate, South Florida Platform, U.S.A. *Geochim. Cosmochim. Acta* **63**: 2529–2546, doi:10.1016/S0016-7037(99)00115-5
- LANGDON, C., AND OTHERS. 2000. Effect of calcium carbonate saturation state on the calcification rate of an experimental coral reef. *Global Biogeochem. Cy.* **14**: 639–654, doi:10.1029/1999GB001195
- LECLERCQ, N., J. P. GATTUSO, AND J. JAUBERT. 2002. Primary production, respiration, and calcification of a coral reef mesocosm under increased CO<sub>2</sub> partial pressure. *Limnol. Oceanogr.* **47**: 558–564, doi:10.4319/lo.2002.47.2.0558
- LEVY, O., Z. DUBINSKY, K. SCHNEIDER, Y. ACHITUV, D. ZAKAI, AND M. Y. GORBUNOV. 2004. Diurnal hysteresis in coral photosynthesis. *Mar. Ecol. Prog. Ser.* **268**: 105–117, doi:10.3354/meps268105
- MEHRBACH, C., C. CULBERSON, J. HAWLEY, AND R. PYTKOWICZ. 1973. Measurement of the apparent dissociation constants of carbonic acid in seawater at atmospheric pressure. *Limnol. Oceanogr.* **18**: 897–907, doi:10.4319/lo.1973.18.6.0897
- MILLIMAN, J., AND A. DROXLER. 1996. Neritic and pelagic carbonate sedimentation in the marine environment: Ignorance is not bliss. *Geol. Rundsch.* **85**: 496–504, doi:10.1007/BF02369004
- MORSE, J. W., A. J. ANDERSSON, AND F. T. MACKENZIE. 2006. Initial responses of carbonate-rich shelf sediments to rising atmospheric PCO<sub>2</sub> and “ocean acidification”: Role of high Mg-calcites. *Geochim. Cosmochim. Acta* **70**: 5814–5830, doi:10.1016/j.gca.2006.08.017
- , AND R. S. ARVIDSON. 2002. The dissolution kinetics of major sedimentary carbonate minerals. *Earth-Sci. Rev.* **58**: 51–84, doi:10.1016/S0012-8252(01)00083-6
- NAKAMURA, T., AND T. NAKAMORI. 2009. Estimation of photosynthesis and calcification rates at a fringing reef by accounting for diurnal variations and the zonation of coral

- reef communities on reef flat and slope: A case study for the Shiraho Reef, Ishigaki Island, southwest Japan. *Coral Reefs* **28**: 229–250, doi:10.1007/s00338-008-0454-8
- OAKES, J. M., B. D. EYRE, D. J. ROSS, AND S. D. TURNER. 2010. Stable isotopes trace estuarine transformations of carbon and nitrogen from primary- and secondary-treated paper and pulp mill effluent. *Environ. Sci. Technol.* **44**: 7411–7417, doi:10.1021/es101789v
- PEARSE, V. B., AND L. MUSCATINE. 1971. Role of symbiotic algae (zooxanthellae) in coral calcification. *Biol. Bull.* **141**: 350–363, doi:10.2307/1540123
- PIERROT, D., E. LEWIS, AND D. W. R. WALLACE. 2006. MS Excel program developed for CO<sub>2</sub> system calculations. Carbon Dioxide Information Analysis Center, Oak Ridge National Laboratory.
- RAO, A. M. F., L. POLERECKY, D. IONESCU, F. J. R. MEYSMAN, AND D. DE BEER. 2012. The influence of pore-water advection, benthic photosynthesis, and respiration on calcium carbonate dynamics in reef sands. *Limnol. Oceanogr.* **57**: 809–825, doi:10.4319/lo.2012.57.3.0809
- RASHEED, M., C. WILD, U. FRANKE, AND M. HUETTEL. 2004. Benthic photosynthesis and oxygen consumption in permeable carbonate sediments at Heron Island, Great Barrier Reef, Australia. *Estuar. Coast. Shelf Sci.* **59**: 139–150, doi:10.1016/j.ecss.2003.08.013
- SANTOS, I. R., D. ERLER, D. TAIT, AND B. D. EYRE. 2010. Breathing of a coral cay: Tracing tidally driven seawater recirculation in permeable coral reef sediments. *J. Geophys. Res.* **115**: C12010, doi:10.1029/2010JC006510
- , B. D. EYRE, AND M. HUETTEL. 2012. The driving forces of porewater and groundwater flow in permeable coastal sediments: A review. *Estuar. Coast. Shelf Sci.* **98**: 1–15, doi:10.1016/j.ecss.2011.10.024
- , R. N. GLUD, D. MAHER, D. ERLER, AND B. D. EYRE. 2011. Diel coral reef acidification driven by porewater advection in permeable carbonate sands, Heron Island, Great Barrier Reef. *Geophys. Res. Lett.* **38**: L03604, doi:10.1029/2010GL046053
- SHAMBERGER, K. E. F., AND OTHERS. 2011. Calcification and organic production on a Hawaiian coral reef. *Mar. Chem.* **127**: 64–75, doi:10.1016/j.marchem.2011.08.003
- VERON, J. E. N. 2011. Ocean acidification and coral reefs: An emerging big picture. *Diversity* **3**: 262–274, doi:10.3390/d3020262
- WEBER, J. N., AND P. M. J. WOODHEAD. 1969. Factors affecting the carbon and oxygen isotopic composition of marine carbonate sediments—II. Heron Island, Great Barrier Reef, Australia. *Geochim. Cosmochim. Acta* **33**: 19–38, doi:10.1016/0016-7037(69)90090-8
- WERNER, U., AND OTHERS. 2008. Microbial photosynthesis in coral reef sediments (Heron Reef, Australia). *Estuar. Coast. Shelf Sci.* **76**: 876–888, doi:10.1016/j.ecss.2007.08.015
- WILD, C., M. HUETTEL, A. KLUETER, S. G. KREMB, M. Y. M. RASHEED, AND B. B. JORGENSEN. 2004a. Coral mucus functions as an energy carrier and particle trap in the reef ecosystem. *Nature* **428**: 66–70, doi:10.1038/nature02344
- , R. TOLLRIAN, AND M. HUETTEL. 2004b. Rapid recycling of coral mass-spawning products in permeable reef sediments. *Mar. Ecol. Prog. Ser.* **271**: 159–166, doi:10.3354/meps271159
- YATES, K., AND R. HALLEY. 2003. Measuring coral reef community metabolism using new benthic chamber technology. *Coral Reefs* **22**: 247–255, doi:10.1007/s00338-003-0314-5
- , AND ———. 2006. Diurnal variation in rates of calcification and carbonate sediment dissolution in Florida Bay. *Estuar. Coasts* **29**: 24–39.
- ZEEBE, R. E., AND D. WOLF-GLADROW. 2001. CO<sub>2</sub> in seawater: Equilibrium, kinetics, isotopes. Elsevier Oceanography Series.

Associate editor: H. Maurice Valett

Received: 06 March 2012

Accepted: 26 July 2012

Amended: 16 August 2012